Pressure balance in a lower collisionality, attached tokamak scrape-off layer

R.M. Churchill[a], C.S. Chang[a], S. Ku[a], R. Hager[a], R. Maingi[a], D.P. Stotler[a], H. Qin[a]

[a] *Princeton Plasma Physics Laboratory, 100 Stellarator Road, Princeton, NJ 08540, USA*

Abstract

Previously the gyrokinetic neoclassical code XGCa found that the pressure balance (or momentum balance) in the diverted scrape-off layer (SOL) does not follow that from the fluid description based on the Chew-Goldberger-Low (CGL) theory. In this paper a gyrofluid equation with gyrokinetic code closure is derived for pressure balance (or momentum balance) in a tokamak SOL, for use in interpreting this difference. The new pressure balance equation allows identifying from the XGCa code results which physical processes dominate the setting of pressure variation in the scrape-off layer. This pressure balance equation is applied to the simulation of a DIII-D H-mode discharge, with a lower ion collisionality in the SOL, and the Coulomb and atomic collisions are not strong enough to yield a detached divertor plasma. It is found that the total pressure balance is much better matched using the gyrofluid equation. Electrons are shown to be dominantly adiabatic, while ions have multiple contributions to pressure balance, including terms originating from particle drifts. These results show that in strong gradient, low collisionality regions of the SOL, the typical fluid reductions miss important effects captured in the gyrokinetic model.

1. Introduction

Predicting scrape-off layer (SOL) divertor pressure based on upstream pressure (or vice-versa) remains a key need to ensure future fusion devices can achieve the high global pressure needed for a burning plasma while limiting the heat and particle fluxes to material surfaces to acceptable levels. More and more, complex simulation codes are being turned to with the goal of including the multiphysics needed to accurately simulate the SOL. Understanding the relative importance of various physics included in these complex simulations is a challenging but important task.

Kotov and Reiter [1] and a recent paper by Stangeby[2] recognized this need, to treat these code simulations as 'experiments', which benefit from formatting the simulation results in simple terms. This not only gives insights into the physical processes at work in the simulation, but also serves as a verification check that the code is solving the specified equations. These papers focused on formatting SOL fluid codes (e.g. SOLPS) outputs into two-point modelling (2PM)[3] like expressions, which relate upstream and downstream quantities such as pressure in the SOL. At its base, 2PM is simply derived from a fluid momentum balance, with a number of extensions accounting for particle/momentum/energy sources, cross-field transport, etc.[3]

A simple application of 2PM was done with output from the gyrokinetic neoclassical code XGCa of a lower collisionality, attached divertor DIII-D[4] H-mode discharge[5, 6]. The total pressure downstream did not match at all the simple 2PM expectations of constant total pressure along a flux surface in the SOL, particularly in the near-SOL (here total pressure refers to the static pressure plus dynamic pressure, i.e. $p_{tot} = p + mnu_{\parallel}^2$). Corrections including the Chew-Golderberger-Low (CGL) viscosity approximation[7], and a neutral source term did not resolve the discrepancy[6]. Since this discharge had lower ion collisionality ($\nu_i^* < 1$ in the near-SOL, where $\nu_i^* \approx 10^{-16} L_{\parallel} n_i / T_i^2$), it was thought that kinetic effects could be playing a role. It was obvious that a more thorough expression for the parallel momentum equation based on the gyrokinetic equations of motion in XGCa was needed to determine the physics responsible.

The purpose of this paper is to derive such an expression for the pressure balance in the SOL, utilizing outputs from the XGCa code (note that pressure balance in this context and throughout this paper is really parallel momentum balance). XGCa is a gyrokinetic neoclassical code[8], and as such has many subtleties when forming full fluid equations, due to the need for a pullback transformation on the 5D gyro-center distribution function ($f(\mathbf{X}, v_{\parallel}, v_{\perp}, t)$).

Indeed, previous work[9] attempting to calculate a full pressure tensor including off-diagonal terms (similar to the "pressure tensor unfolding" technique[10]) produced certain large, unbalanced terms which may require higher order terms in the Taylor expansion of the full distribution function in order to enable use. To avoid these issues, we instead in this paper focus on forming gyrofluid equations by directly taking moments of the gyrokinetic equations of motion in XGCa.

Email address: rchurchi@pppl.gov (R.M. Churchill)

2. XGCa

XGCa[8] is a total-f, gyrokinetic neoclassical PIC (particle-in-cell code), focused on edge physics. It shares the same code base as the turbulent version, XGC1[11], with the main difference being XGCa removes turbulence, i.e. only solves for the axisymmetric ($n = 0$) electric potential (and thus requires much less computational power). Highlights of both codes are the use of full magnetic geometry, including X-points and the separatrix, sheath effects through a logical sheath boundary condition[12, 5], recycling neutrals and Monte-Carlo neutral transport module, and natural inclusion of particle drifts at the kinetic level. For this simulation, we will use the electrostatic version and two species only (i.e. no impurities).

The XGC codes use a hybrid Langrangian scheme[13], which uses gyrokinetic equations of motion to push marker particles, based on equations from Littlejohn[14] and Hahm[15]. Here we review the gyrokinetic equation used in XGC, since we will be forming gyrofluid equations from it. The electrostatic gyrokinetic equations of motion used in XGCa are[13, 16]:

$$\begin{array}{l} \partial_t f + \dot{\mathbf{X}} \cdot \nabla f + \dot{v}_\parallel \cdot \partial_{v_\parallel} f = S^*(f) \\ \quad \dot{\mathbf{X}} = \frac{1}{B^*}\left[v_\parallel \mathbf{B}^* + \frac{1}{q}\mathbf{F} \times \hat{\mathbf{b}}\right] \\ \quad \dot{v}_\parallel = \frac{1}{mB^*}\mathbf{B}^* \cdot \mathbf{F} \\ \quad \dot{\mu} = 0 \end{array} \tag{1}$$

where:

$$\begin{array}{rcl} B^* & = & \hat{\mathbf{b}} \cdot \mathbf{B}^* \\ \mathbf{B}^* & = & \mathbf{B} + \frac{m}{q} v_\parallel \nabla \times \hat{\mathbf{b}} \\ \mathbf{F} & = & q\bar{\mathbf{E}} - \mu \nabla B \end{array} \tag{2}$$

Here $f = f(\mathbf{X}, v_\parallel, \mu, t)$ is the gyro-center distribution functions, the over dot is the total time derivative (e.g. $\dot{A} = dA/dt$), $\mathbf{X}$ the particle gyro-center spatial coordinate vector, $v_\parallel$ the particle parallel velocity, $\mu = \frac{1}{2}mv_\perp^2/B$ the magnetic moment, S^* is a source term including collisions, neutrals, heating, torque, etc., $\hat{\mathbf{b}}$ the unit vector along the magnetic field, $\overline{\mathbf{E}} = -\overline{\nabla\Phi}$ is the gyroaveraged electric field[17], which has a perpendicular velocity dependence i.e. $\bar{\mathbf{E}} = \bar{\mathbf{E}}(\mathbf{X}, v_\perp)$, and other variables have their usual meaning. Note importantly that Equation 1 was derived for a $(\mathbf{X}, v_\parallel, \mu, t)$ system, so that e.g. the ∇ operator is performed holding $(v_\parallel, \mu)$ constant.

3. Gyrofluid parallel momentum equation

Gyrofluid formulations have a long history in fusion physics[18, 19, 20, 21]. The basic concept is to take moments of the gyrokinetic equation directly, and thereby derive fluid-like equations for conservation of particles, momentum, energy, etc., which still retain various kinetic effects such as finite Larmor radius (FLR) effects. Usually gyrofluid equations are used in a "predictive" fashion, where closures are selected to deal with higher order moments in the equations. Here the gyrofluid equation we derive will be used in an "interpretive" manner, where we will use the gyro-center distribution function calculated from XGCa to calculate all moments in the gyrofluid equation, avoiding the need for analytic closures, and allowing us to understand terms which are important in the momentum equation (and hence pressure balance).

For ease of taking moments of the gyrokinetic Vlasov equation, we can write Equation 1 in a conservative form:

$$\partial_t \left(B^* f\right) + \nabla \cdot \left(B^* \dot{\mathbf{X}} f\right) + \partial_{v_\parallel}\left(B^* \dot{v}_\parallel f\right) = B^* S(f) \tag{3}$$

where we have used the observation that:

$$\partial_t B^* + \nabla \cdot \left(B^* \dot{\mathbf{X}}\right) + \partial_{v_\parallel}\left(B^* \dot{v}_\parallel\right) = 0 \tag{4}$$

i.e. the gyrokinetic variation of the Liouville Theorem[22]. We now form the gyrofluid parallel momentum equation by multiplying Equation 3 by $mv_\parallel$ and then integrating over velocity space, $\int d^3v = 2\pi \int dv_\parallel dv_\perp v_\perp$. After some algebra, we arrive at the desired gyrofluid parallel momentum equation:

$$\begin{array}{c} \partial_t\left(mnu_\parallel\right) + \hat{\mathbf{b}} \cdot \nabla\left(p_\parallel + mnu_\parallel^2\right) - \left(\hat{\mathbf{b}} \cdot \frac{\nabla B}{B}\right)\left(p_\parallel + mnu_\parallel^2 - p_\perp\right) - \hat{\mathbf{b}} \cdot \langle q\bar{\mathbf{E}}\rangle_f + \\ + \frac{m}{qB}\left[\left(\hat{\mathbf{b}} \cdot \nabla \times \hat{\mathbf{b}}\right)\partial_t\left(p_\parallel + mnu_\parallel^2\right) + \left(\nabla \times \hat{\mathbf{b}}\right) \cdot \left(\nabla\langle mv_\parallel^3\rangle_f - \frac{\nabla B}{B}\langle mv_\parallel^3\rangle_f + \frac{\nabla B}{B}\langle mv_\parallel v_\perp^2\rangle_f - 2\langle v_\parallel q\bar{\mathbf{E}}\rangle_f\right) + \right. \\ \left. + \left(\hat{\mathbf{b}} \times \frac{\nabla B}{B}\right) \cdot \nabla\langle\tfrac{1}{2}mv_\parallel v_\perp^2\rangle_f + \hat{\mathbf{b}} \cdot \nabla \times \langle v_\parallel q\bar{\mathbf{E}}\rangle_f + \frac{\nabla B}{B} \cdot \hat{\mathbf{b}} \times \langle v_\parallel q\bar{\mathbf{E}}\rangle_f\right] = \langle mv_\parallel\rangle_{S^*} + \frac{m}{qB}\left(\hat{\mathbf{b}} \cdot \nabla \times \hat{\mathbf{b}}\right)\left\langle mv_\parallel^2\right\rangle_{S^*} \end{array} \tag{5}$$

the notation $\langle A\rangle_f = \int d\mathbf{v} A f$ is used, and the following definitions for moments:

$$\begin{array}{rlrl} n & = \int d\mathbf{v} f & nu_\parallel & = \int d\mathbf{v} v_\parallel f \\ p_\parallel & = \int d\mathbf{v} m(v_\parallel - u_\parallel)^2 f & p_\perp & = \int d\mathbf{v} \frac{1}{2} m v_\perp^2 f \end{array} \tag{6}$$

The first line of Equation 5 is familiar, it includes the typical time derivative of parallel momentum, the parallel gradient of the total parallel pressure, a parallel viscosity term, and the parallel electric field force. The second and third lines have numerous terms which are presumably smaller in the usual plasma that is close to thermal equilibrium, due to the factor $1/\omega_c = m/qB$, which is the gyroradius or banana width factor. Most of these terms have origins in the particle drifts. The third line also has

terms due to the sources (collisions/neutrals). These terms are responsible for the friction force and neutral drag terms seen in fluid equations. See Appendix A for further comparisons of Equation 5 with typical fluid equations. In the SOL of a non-Maxwellian plasma, especially with tail ions, it will be shown that the terms in the second and third lines can make a significant contribution.

In order to have an expression for the pressure directly, we will perform a line integral along a flux surface in the parallel direction, $\int d\ell_\parallel$, from a point downstream ($\ell_\parallel = 0$) to a point upstream ($\ell_\parallel = x$). Applying this integral to Equation 5, and rearranging terms, we arrive at an equation similar to past equations[6]:

$$\frac{p_{\parallel,tot}|_{\ell_\parallel=x}}{p_{\parallel,tot}|_{\ell_\parallel=0}} + \sum_j F_j = 1 \tag{7}$$

where we have written $p_{\parallel,tot} = p_\parallel + mnu_\parallel^2$, and where each F_j represents the integral of one of the terms from Equation 5 (excluding the parallel gradient of pressure term), normalized to $p_{\parallel,tot}|_{\ell_\parallel=0}$. The F_j terms are as follows:

$$\begin{aligned}
F_{\partial_t} &= \frac{-\int_0^x d\ell_\parallel \partial_t(mnu_\parallel) + \frac{m}{qB}(\hat{\mathbf{b}}\cdot\nabla\times\hat{\mathbf{b}})\partial_t(p_\parallel + mnu_\parallel^2)}{p_{\parallel,tot}|_{\ell_\parallel=0}} \\
F_{E_\parallel} &= \frac{-\int_0^x d\ell_\parallel \hat{\mathbf{b}}\cdot\langle\bar{\mathbf{E}}\rangle_f}{p_{\parallel,tot}|_{\ell_\parallel=0}} \\
F_{\nabla mv_\parallel^2} &= \frac{\int_0^x d\ell_\parallel \frac{m}{qB}\left(\nabla\times\hat{\mathbf{b}}\right)\cdot\nabla\langle mv_\parallel^3\rangle_f}{p_{\parallel,tot}|_{\ell_\parallel=0}} \\
F_{2\langle v_\parallel q\bar{\mathbf{E}}\rangle_f} &= \frac{-\int_0^x d\ell_\parallel \frac{m}{qB}\left(\nabla\times\hat{\mathbf{b}}\right)\cdot 2\langle v_\parallel q\bar{\mathbf{E}}\rangle_f}{p_{\parallel,tot}|_{\ell_\parallel=0}} \\
F_{\hat{\mathbf{b}}\cdot\nabla\times\left\langle v_\parallel q\bar{\mathbf{E}}\right\rangle_f} &= \frac{\int_0^x d\ell_\parallel \frac{m}{qB}\left(\hat{\mathbf{b}}\times\frac{\nabla B}{B}\right)\cdot\hat{\mathbf{b}}\cdot\nabla\times\left\langle v_\parallel q\bar{\mathbf{E}}\right\rangle_f}{p_{\parallel,tot}|_{\ell_\parallel=0}}
\end{aligned}$$

$$\begin{aligned}
F_{visc} &= \frac{-\int_0^x d\ell_\parallel\left(\hat{\mathbf{b}}\cdot\frac{\nabla B}{B}\right)\left(p_\parallel + mnu_\parallel^2 - p_\perp\right)}{p_{\parallel,tot}|_{\ell_\parallel=0}} \\
F_{source} &= \frac{\int_0^x d\ell_\parallel \left\langle mv_\parallel\right\rangle_S + \frac{m}{qB}\left(\hat{\mathbf{b}}\cdot\nabla\times\hat{\mathbf{b}}\right)\left\langle mv_\parallel^2\right\rangle_S}{p_{\parallel,tot}|_{\ell_\parallel=0}} \\
F_{\left(\nabla\times\hat{\mathbf{b}}\right)\cdot\frac{\nabla B}{B}} &= \frac{\int_0^x d\ell_\parallel \frac{m}{qB}\left(\nabla\times\hat{\mathbf{b}}\right)\cdot\frac{\nabla B}{B}\left(\langle mv_\parallel v_\perp^2\rangle_f - \langle mv_\parallel^3\rangle_f\right)}{p_{\parallel,tot}|_{\ell_\parallel=0}} \\
F_{\nabla\langle\frac{1}{2}mv_\parallel v_\perp^2\rangle_f} &= \frac{\int_0^x d\ell_\parallel \frac{m}{qB}\left(\hat{\mathbf{b}}\times\frac{\nabla B}{B}\right)\cdot\nabla\langle\frac{1}{2}mv_\parallel v_\perp^2\rangle_f}{p_{\parallel,tot}|_{\ell_\parallel=0}}
\end{aligned} \tag{8}$$

4. Gyrofluid pressure balance in XGCa

We now use the integrated gyrofluid momentum equation (Equation 7) with the gyro-center distribution functions, f_e and f_i, and field quantities from an XGCa simulation of a lower collisionality H-mode DIII-D discharge, in which electron temperature is high enough to avoid detachment of the divertor plasma. This is the same discharge and simulation setup as Ref. [5], however the simulation has been redone to include additional diagnostic outputs useful for calculating Equation 7, such as the source term and gyroaveraged electric field.

The sum over species (electron and ion) of the pressure and parallel momentum equation terms (the LHS of Equation 7) along various flux surfaces in the SOL are plotted in Figure 1. For comparison, the total pressure normalized to the target total pressure, $\frac{p_{tot}|_{\ell_\parallel=x}}{p_{tot}|_{\ell_\parallel=0}}$, is plotted also in Figure 1. Complete pressure balance would result in these plots being one everywhere (unity line). For the total pressure ratio only, it can be seen that a large 2-3x momentum imbalance is observed, worsening as we go further upstream from the divertor plate. In contrast, the gyrofluid formulation has only a 10-30% maximum deviation from the unity line, depending on the flux surface, over the the whole distance between the divertor plates ($Z \approx -1.25$m) and the outboard midplane (Z=0m). This is a significant improvement over the CGL based fluid equation, and shows that the gyrofluid equation (Eq. 5) correctly represents the underlying XGCa equations of motion. The up to 30% error may still not be satisfactory for some SOL physics analysis and further improvement will be attempted in the future.

Now that we have an equation which accurately describes the pressure balance in the SOL, we can look at the individual F_j terms which make up Equation 7 and 8 to determine which terms are the most important. For ease of visualization, we will plot normalized F_j factors:

$$F_{j,norm} = \frac{F_j}{\sum_k |F_k|} \tag{9}$$

where the sum over k is all the terms in Equation 7, including a factor $F_{p_\parallel} = \frac{p_{\parallel,tot}|_{\ell_\parallel=x}}{p_{\parallel,tot}|_{\ell_\parallel=0}} - 1$. By stacking these $F_{j,norm}$ terms for a particular flux surface in a visualization, we can easily check if momentum balances at a particular flux surface, ψ_N, if the vertical sum is equal to 0. Additionally, the normalization allows a quick check whether the positive and negative contributions are at +0.5 and -0.5 respectively to have momentum balance, and allows for a level comparison among many flux surfaces.

We now plot in Figure 2 the normalized factors from Equation 9, first for the electron gyrofluid momentum equation. The integration is done over the LFS divertor ($x = 0$) to the LFS midplane ($x = x_{midplane}$) for each flux surface, and a range of flux surfaces $1.004 \leq \psi_N \leq 1.042$ are plotted. As can be seen, the electrons are dominantly adiabatic in the present neoclassical SOL, with the parallel pressure being balanced by the parallel electric field force. The source terms coming from collisions/neutrals becomes increasingly important in the far-SOL, but still makes up only about 10% of the electron momentum balance.

Contrast the simple electron picture now with the ions in Figure 3. There is again a large parallel pressure imbalance, but instead of the simple momentum balance with parallel electric field force, there are various other terms which are important. We now comment on several of these.

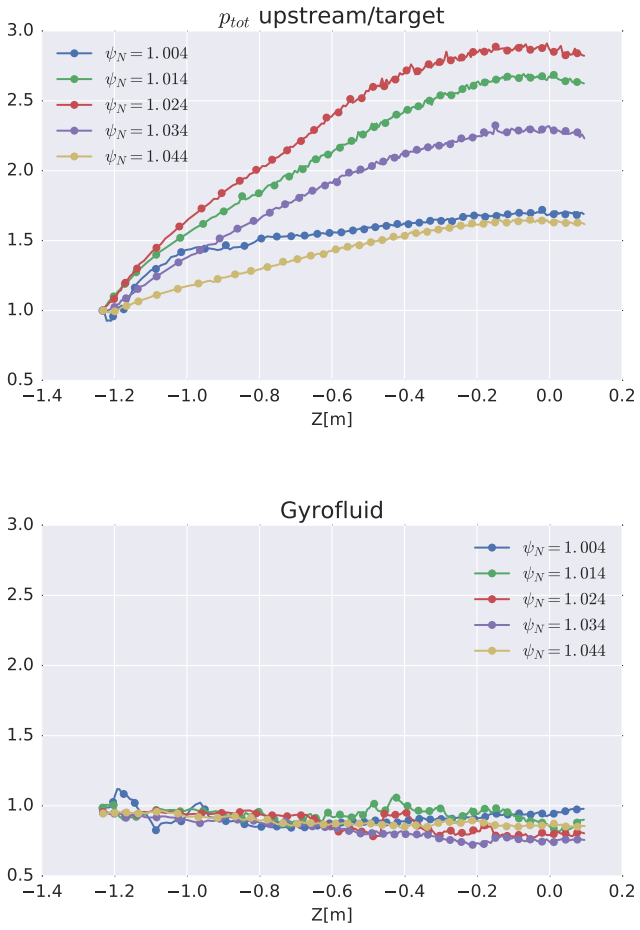

Figure 1: Pressure balance in the SOL, plotted along flux surfaces (plotted versus Z, the normal cylindrical coordinate height coordinate, at each point on the flux surface). The top figure shows the ratio of upstream total pressure to target total pressure, and the bottom figure shows the same but with the $\sum_j F_j$ terms from the gyrofluid parallel momentum equation (Equation 7) included.

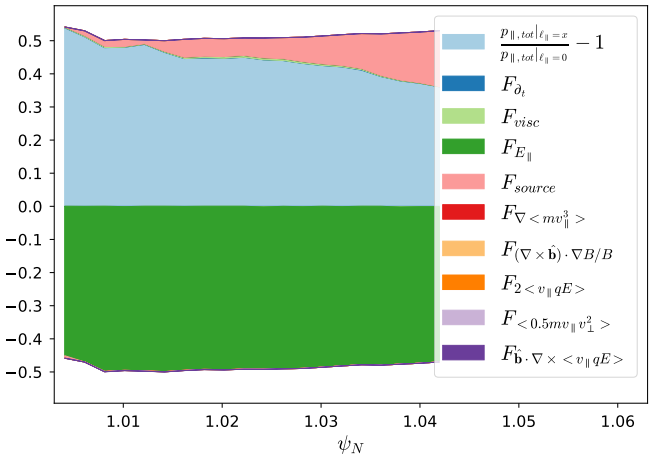

Figure 2: Individual terms from the electron pressure balance (Equation 7). As seen, the electrons are dominantly adiabatic, with the parallel electric field force balancing the parallel pressure.

The largest ion momentum loss terms, which dominantly counteract the large total parallel ion pressure imbalance, are (1) parallel ion viscosity, and (2) gradient of parallel ion energy flux terms, which have origins in the net parallel momentum into or out of the flux surface carried by the particle magnetic cross-field drifts (a similar term $\nabla \cdot \left\langle m v_\parallel \mathbf{v}_{dr} \right\rangle_f$ can be seen in Chankin, et. al.[10]). Additionally, there is some modest momentum loss due to collisions/neutral sources, contributing dominantly in the far-SOL (similar to the electrons).

The largest parallel ion momentum gain terms, besides the parallel pressure term, are dominantly related to the electric field. Its important to note that the electric field in Eq. 5 is the gyroaveraged electric field, which is a nonlocal field. Because higher energy ions have a larger Larmor radius, they sample or feel the electric field far from their gyro-center, and this is captured in the gyroaveraged electric field, since it has perpendicular velocity dependence, $\bar{\mathbf{E}} = \bar{\mathbf{E}}(\mathbf{X}, v_\perp)$. When the electric field is changing over a short spatial distance, such as near the separatrix where the typical H-mode E_r well is just inside, the electric field felt by higher energy ions will be very different than for lower energy ions. For the two small electric field terms in the momentum equation ($\langle q\bar{\mathbf{E}} \rangle_f$ and $\langle v_\parallel q\bar{\mathbf{E}} \rangle_f$), using either the local ($\mathbf{E} = \bar{\mathbf{E}}(\mathbf{X}, 0)$) or gyroaveraged electric field gives close to the same results, due to not involving gradients on the moments involving the gyroaveraged electric field. However, for the term $\hat{\mathbf{b}} \cdot \nabla \times \langle v_\parallel q\bar{\mathbf{E}} \rangle_f$, its important to realize that this term is a momentum *gain* near the separatrix because of the gyroaveraged electric field; using the local electric field only, this term would actually be a momentum *loss* near the separatrix, and lead to a large apparent momentum imbalance in the simulation. This shows an important kinetic effect which is captured in these gyrokinetic simulations, and which has a sizeable impact on the parallel momentum balance in the near-SOL.

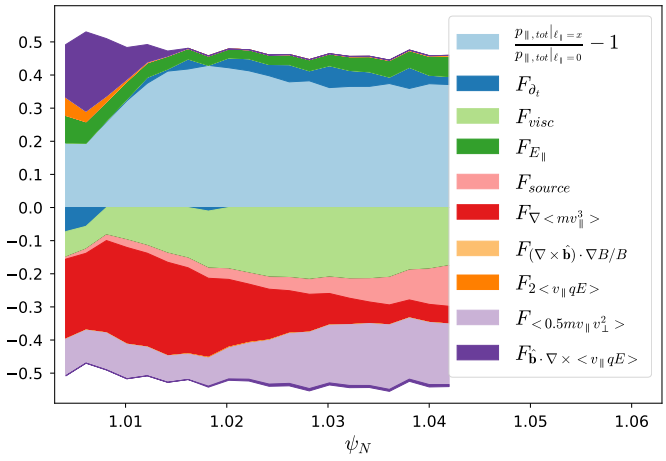

Figure 3: Individual terms from the ion pressure balance (Equation 7). Many terms are important and sizeable besides the parallel pressure, including ion parallel viscosity, and terms resulting from particle drifts.

5. Conclusions

A gyrofluid parallel momentum equation with gyrokinetic code closure has been derived from the XGCa gyrokinetic neoclassical equations of motion, for use in interpreting the relative importance of terms in setting the pressure balance in the SOL. As was shown, for this discharge the electrons are dominantly adiabatic in the SOL, while the ions have significant contributions from parallel momentum gain/loss due to magnetic and $E \times B$ drifts. Accounting for all terms brings total parallel pressure balance much closer to the expected unity level.

One important takeaway from this study is that drifts are very important to take into account, even in the SOL where they can often be neglected in fluid modeling. As seen in this paper, even in simple pressure balance, where its usually assumed the pressure itself with the ion inertia are the dominant terms, the effect of drifts can play an integral role. Caution must be used when not including drifts, especially in the near-SOL.

A second important takeaway is the effect of non-Maxwellian ions on the momentum balance, and the large effect of the parallel ion viscosity, coming from the difference in parallel and perpendicular ion temperatures. In general, ion temperature and flows are difficult quantities to measure accurately in the SOL of fusion experiments, but increased diagnostic efforts should be made to accurately measure the ion temperature and flows and thus enable a better understanding of the role of ions in the SOL.

Future work will simulate varying discharges in higher collisional regimes, including detached divertor discharges, for determining how these kinetic effects will be modified in more fluid-like conditions. Inclusion of turbulence is also left as a future work.

6. Acknowledgments

The main author would like to thank Greg Hammett for helpful discussions and insights. This material is based upon work supported by the U.S. Department of Energy, Office of Science, Office of Fusion Energy Sciences, under AC02-09CH11466 and DE-FC02-04ER54698. This research used resources of the National Energy Research Scientific Computing Center (NERSC), a U.S. Department of Energy Office of Science User Facility operated under Contract No. DE-AC02-05CH11231.

Appendix A: Connection with typical fluid equations

We can rewrite the Eq. 5 to be closer to the typical fluid equations used in e.g. Braginskii formulations. First, the parallel pressure gradient and parallel viscosity piece can be rewritten to be in the form of total pressure and the typical form for the parallel viscous force, as was done in Ref. [9]:

$$\hat{\mathbf{b}}\cdot\nabla\left(p_\parallel\right) - \hat{\mathbf{b}}\cdot\frac{\nabla B}{B}\left(p_\parallel - p_\perp\right) \quad = \quad \hat{\mathbf{b}}\cdot\nabla\left(p\right) + \left(\hat{\mathbf{b}}\cdot\nabla\cdot\pi\right)_0 \tag{10}$$

where we've used the definitions for static pressure $p = (p_\parallel + 2p_\perp)/3$ and the lowest-order parallel viscous force resulting from a diagonal pressure tensor:

$$\left(\hat{\mathbf{b}}\cdot\nabla\cdot\pi\right)_0 = \frac{2}{3}\hat{\mathbf{b}}\cdot\nabla(p_\parallel - p_\perp) - \hat{\mathbf{b}}\cdot\frac{\nabla B}{B}(p_\parallel - p_\perp)$$

The second and part of the third lines in Eq. 5, those having a prefix of $1/\omega_c$, are all higher order viscous force related terms, which have origins in a term like $\langle mv_\parallel \mathbf{v}_{dr}\rangle_f$. These terms are off-diagonal components of the pressure stress tensor. Formally in the $1/\omega_c$ ordering, these terms appear as the first order terms. However, in a non-Maxwellian and anisotropic plasma with strong plasma gradient, they are not small. We will group them then in a term $\left(\hat{b}\cdot\nabla\cdot\pi\right)_1$.

The source term, $\langle mv_\parallel\rangle_{S^*} + \frac{m}{qB}\left(\hat{\mathbf{b}}\cdot\nabla\times\hat{\mathbf{b}}\right)\left\langle mv_\parallel^2\right\rangle_{S^*}$, which includes collisions and neutrals, can be written in the typical form of a friction force $\hat{\mathbf{b}}\cdot\mathbf{R} = \sum_a \int d\mathbf{v} m v_\parallel C(f, f_a)$ and a neutral force term $\hat{\mathbf{b}}\cdot\mathbf{F}_n = m u_\parallel n_n(\nu_{ion} + \nu_{cx})$.

Putting this all together, we arrive at the equation:

$$\partial_t\left(mnu_\parallel\right) + \hat{\mathbf{b}}\cdot\nabla\left(mnu_\parallel^2\right) - \hat{\mathbf{b}}\cdot\frac{\nabla B}{B}\left(mnu_\parallel^2\right) + \hat{\mathbf{b}}\cdot\nabla p + \left(\hat{\mathbf{b}}\cdot\nabla\cdot\pi\right)_0 - \hat{\mathbf{b}}\cdot\left\langle q\bar{\mathbf{E}}\right\rangle_f + \left(\hat{\mathbf{b}}\cdot\nabla\cdot\pi\right)_1 = \hat{\mathbf{b}}\cdot\mathbf{R} + \hat{\mathbf{b}}\cdot\mathbf{F}_n \tag{11}$$

References

[1] V. Kotov, D. Reiter, Two-point analysis of the numerical modelling of detached divertor plasmas, Plasma Phys. Control. Fusion 51 (11) (2009) 115002. doi:10.1088/0741-3335/51/11/115002.
URL http://stacks.iop.org/0741-3335/51/i=11/a=115002

[2] P. C. Stangeby, Basic physical processes and reduced models for plasma detachment, Plasma Phys. Control. Fusion 60 (4) (2018) 044022. doi:10.1088/1361-6587/aaacf6.
URL http://stacks.iop.org/0741-3335/60/i=4/a=044022?key=crossref.34a2c3a50b5467333f4072ed223e94b7

[3] P. Stangeby, The Plasma Boundary of Magnetic Fusion Devices, Institute of Physics Publishing, Bristol, 2000.

[4] J. L. Luxon, T. C. Simonen, R. D. Stambaugh, Overview of the DIII-D Fusion Science program, Fusion Sci. Technol. 48 (2) (2005) 807–827.

[5] R. Churchill, J. Canik, C. Chang, R. Hager, A. Leonard, R. Maingi, R. Nazikian, D. Stotler, Kinetic simulations of scrape-off layer physics in the DIII-D tokamak, Nucl. Mater. Energy 12 (2017) 978–983. doi:10.1016/j.nme.2016.12.013.
URL http://linkinghub.elsevier.com/retrieve/pii/S2352179116302101

[6] R. Churchill, J. Canik, C. Chang, R. Hager, A. Leonard, R. Maingi, R. Nazikian, D. Stotler, Total fluid pressure imbalance in the scrape-off layer of tokamak plasmas, Nucl. Fusion 57 (4) (2017) 046029. doi:10.1088/1741-4326/aa5fb1.
URL http://stacks.iop.org/0029-5515/57/i=4/a=046029?key=crossref.c8912c7beec19d66c3b076c51d024c1c

[7] G. F. Chew, M. L. Goldberger, F. E. Low, The Boltzmann Equation and the One-Fluid Hydromagnetic Equations in the Absence of Particle Collisions, Proc. R. Soc. A Math. Phys. Eng. Sci. 236 (1204) (1956) 112–118. doi:10.1098/rspa.1956.0116.
URL http://rspa.royalsocietypublishing.org/cgi/doi/10.1098/rspa.1956.0116

[8] R. Hager, C. S. Chang, Gyrokinetic neoclassical study of the bootstrap current in the tokamak edge pedestal with fully nonlinear Coulomb collisions, Phys. Plasmas 23 (4) (2016) 042503. doi:10.1063/1.4945615.
URL http://scitation.aip.org/content/aip/journal/pop/23/4/10.1063/1.4945615

[9] R. Churchill, C. Chang, R. Hager, On pressure balance in a low collisionality tokamak scrape-off layer, Bull. Am. Phys. Soc. Volume 62,.
URL https://meetings.aps.org/Meeting/DPP17/Session/PP11.74

[10] A. Chankin, P. Stangeby, Particle and parallel momentum balance equations with inclusion of drifts, for modelling strong-to weakly-collisional edge plasmas, Nucl. Fusion 46 (12) (2006) 975–993. doi:Doi10.1088/0029-5515/46/12/001.
URL http://iopscience.iop.org/article/10.1088/0029-5515/46/12/001

[11] S. Ku, C. Chang, P. Diamond, Full-f gyrokinetic particle simulation of centrally heated global ITG turbulence from magnetic axis to edge pedestal top in a realistic tokamak geometry, Nucl. Fusion 49 (11) (2009) 115021. doi:10.1088/0029-5515/49/11/115021.
URL http://iopscience.iop.org/0029-5515/49/11/115021

[12] S. Parker, R. Procassini, C. Birdsall, B. Cohen, A Suitable Boundary Condition for Bounded Plasma Simulation without Sheath Resolution, J. Comput. Phys. 104 (1) (1993) 41–49. doi:10.1006/jcph.1993.1005.
URL http://www.sciencedirect.com/science/article/pii/S0021999183710053

[13] S. Ku, R. Hager, C. Chang, J. Kwon, S. Parker, A new hybrid-Lagrangian numerical scheme for gyrokinetic simulation of tokamak edge plasma, J. Comput. Phys. 315 (2016) 467–475. doi:10.1016/j.jcp.2016.03.062.
URL http://linkinghub.elsevier.com/retrieve/pii/S0021999116300274

[14] R. G. Littlejohn, Variational principles of guiding centre motion, J. Plasma Phys. 29 (01) (1983) 111. doi:10.1017/S002237780000060X.
URL http://www.journals.cambridge.org/abstract{_}S002237780000060X

[15] T. S. Hahm, Nonlinear gyrokinetic equations for tokamak microturbulence, Phys. Fluids 31 (9) (1988) 2670–2673. doi:10.1063/1.866544.
URL http://scitation.aip.org/content/aip/journal/pof1/31/9/10.1063/1.866544

[16] S. Ku, C. S. Chang, R. Hager, R. M. Churchill, G. R. Tynan, I. Cziegler, M. Greenwald, J. Hughes, S. E. Parker, M. F. Adams, E. D'Azevedo, P. Worley, A fast low-to-high confinement mode bifurcation dynamics in the boundary-plasma gyrokinetic code XGC1, Phys. Plasmas 25 (5) (2018) 056107. doi:10.1063/1.5020792.
URL http://aip.scitation.org/doi/10.1063/1.5020792

[17] W. Lee, Gyrokinetic particle simulation model, J. Comput. Phys. 72 (1) (1987) 243–269. doi:10.1016/0021-9991(87)90080-5.
URL http://www.sciencedirect.com/science/article/pii/0021999187900805

[18] G. W. Hammett, F. W. Perkins, Fluid moment models for Landau damping with application to the ion-temperature-gradient instability, Phys. Rev. Lett. 64 (25) (1990) 3019–3022. doi:10.1103/PhysRevLett.64.3019.
URL https://link.aps.org/doi/10.1103/PhysRevLett.64.3019

[19] M. A. Beer, G. W. Hammett, G. Rewoldt, E. J. Synakowski, M. C. Zarnstorff, W. Dorland, Gyrofluid simulations of turbulence suppression in reversed-shear experiments on the Tokamak Fusion Test Reactor, Phys. Plasmas 4 (5) (1997) 1792. doi:10.1063/1.872279.
URL https://aip.scitation.org/doi/10.1063/1.872279

[20] P. B. Snyder, Gyrofluid Theory and Simulation of Electromagnetic Turbulence and Transport in Tokamak Plasmas, Ph.D. thesis, Princeton University (1999).
URL https://w3.pppl.gov/{~}hammett/gyrofluid/papers/1999/thesis.pdf

[21] W. Dorland, G. W. Hammett, Gyrofluid turbulence models with kinetic effects, Phys. Fluids B Plasma Phys. 5 (3) (1993) 812–835. doi:10.1063/1.860934.
URL http://aip.scitation.org/doi/10.1063/1.860934

[22] A. Brizard, T. Hahm, Foundations of nonlinear gyrokinetic theory, Rev. Mod. Phys. 79 (2) (2007) 421–468. doi:10.1103/RevModPhys.79.421.
URL http://link.aps.org/doi/10.1103/RevModPhys.79.421